Supporting Information for

"Ligand-induced Dependence of Charge Transfer in Nanotube – Quantum Dot Heterostructures"

Lei Wang,[a] Jinkyu Han,[b] Bryan Sundahl,[c] Scott Thornton,[c] Yuqi Zhu,[d] Ruiping Zhou,[d] Cherno Jaye,[e] Haiqing Liu,[a] Zhuo-Qun Li,[f] Gordon T. Taylor,[f] Daniel A. Fischer,[e] Joerg Appenzeller,[d] Robert J. Harrison,[c,g] and Stanislaus S. Wong[a,b,*]

Email: stanislaus.wong@stonybrook.edu; sswong@bnl.gov

[a]Department of Chemistry, State University of New York at Stony Brook, Stony Brook, NY 11794-3400

[b]Condensed Matter Physics and Materials Sciences Division, Brookhaven National Laboratory, Building 480, Upton, NY 11973

[c]Institute of Advanced Computational Science, State University of New York at Stony Brook, Stony Brook, NY 11794 USA

[d]Department of Electrical and Computer Engineering and Birck Nanotechnology Center, Purdue University, West Lafayette, Indiana 47907

[e]Material Measurement Laboratory, National Institute of Standards and Technology, Gaithersburg, Maryland 20889

[f]School of Marine and Atmospheric Sciences, State University of New York at Stony Brook, Stony Brook, NY 11794-5000

[g]Computational Science Center, Brookhaven National Laboratory, Upton, NY 11973 USA

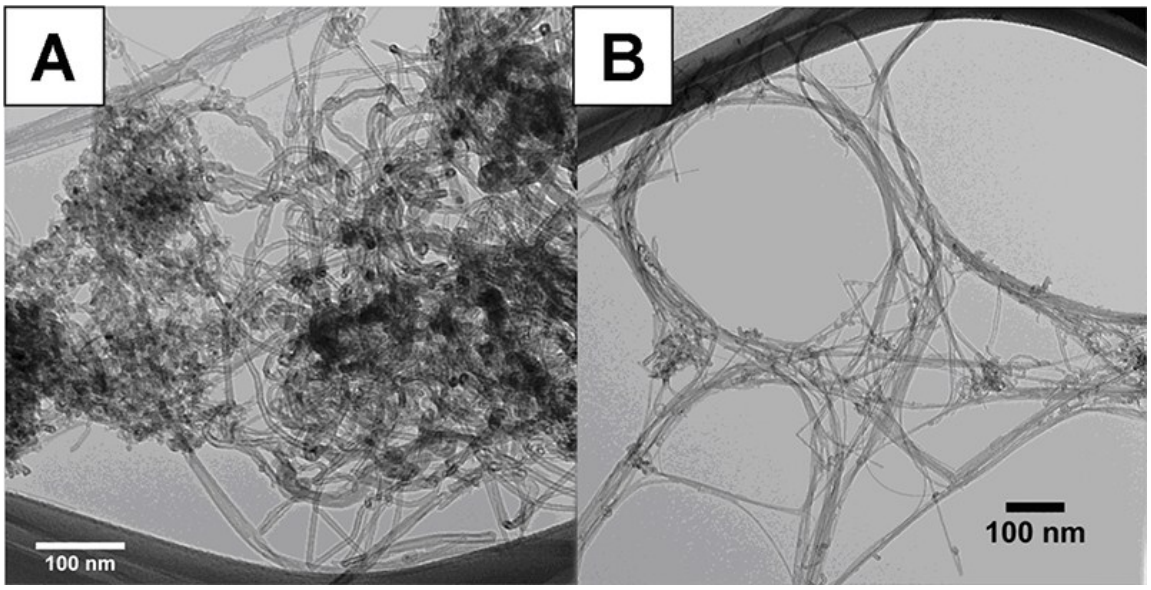

Figure S1. TEM images of (A) pristine and (B) purified DWNTs.

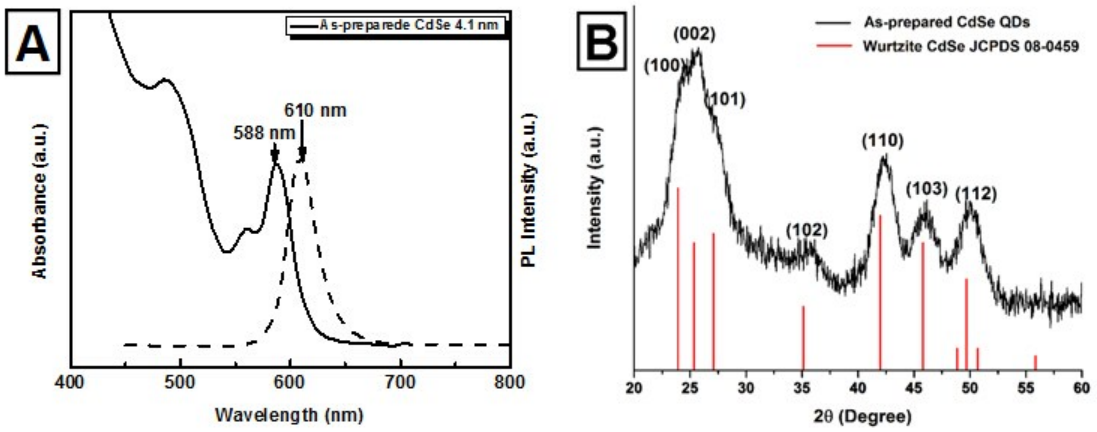

Figure S2. (A) UV-visible and photoluminescence spectra of as-prepared CdSe QDs possessing average diameter of 4.1 nm. (B) XRD patterns of as-prepared CdSe QDs (measuring 4.1 nm in diameter). The corresponding literature database standard (JCPDS #08-0459) is shown immediately below and is highlighted in red.

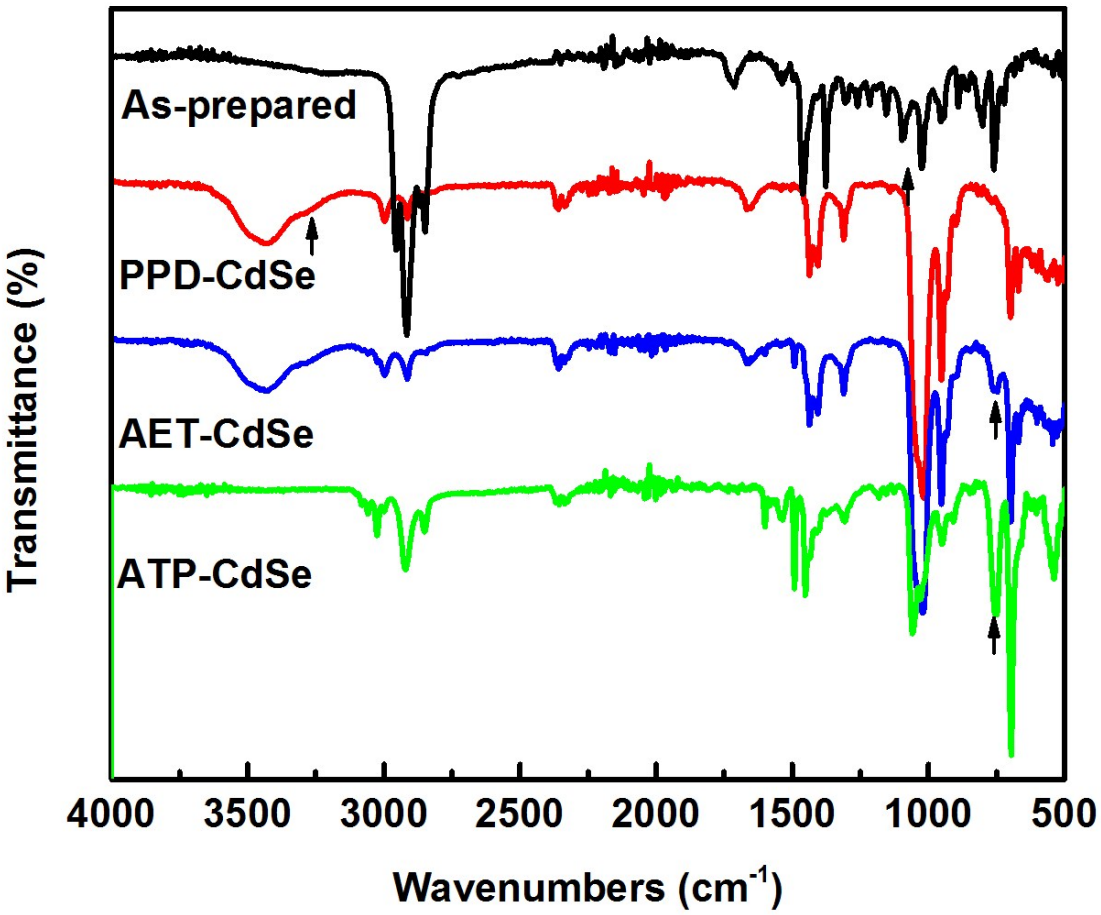

Figure S3. FT-IR spectra of as-prepared, PPD, AET and ATP-capped CdSe QDs possessing average diameters of 4.1 nm, respectively.

Comments on IR Characterization.

The presence of the various ligand terminated moieties (i.e. PPD, AET, and ATP) on the CdSe QD surfaces expected after ligand exchange was confirmed by FT-IR analysis, as shown in Figure S3. Specifically, for the as-prepared CdSe QDs, the surface capping agent is TOPO.[1] The small sharp peak near 1151 cm^{-1} can be assigned to the P=O stretch mode, corresponding to free TOPO molecules.[2] Concomitant with the small peak associated with the unbound and free TOPO, a more significant broadened peak was observed at ~1097 cm^{-1}, which can be assigned to the bound TOPO molecules, since a red-shift of the P=O stretching frequency is often observed when TOPO is coordinated onto the QD surface[3] through the occupation of bridging sites on the Cd surface.[4, 5]

Such a distinctive peak is essentially absent in ligand-exchanged PPD, AET, and ATP-capped CdSe QDs, respectively, implying not only a practically complete removal of the surface TOPO capping agents but also a successful ligand exchange process. Significantly, in the case of CdSe QDs capped with thiol ligands such as AET and ATP, after the respective ligand exchange reactions involved, the absence of a distinctive R-SH peak near 2400-2500 cm^{-1} suggests that all thiol pendant moieties in these ligands are likely to be completely bound onto the external surfaces of the CdSe QDs.[3, 6] Moreover, the two N-H stretching bands for free PPD species initially located near 3400-3300 and 3330-3250 cm^{-1}, respectively, are strongly broadened and red-shifted to 3280 cm^{-1}, in the corresponding spectra of the ligand-capped dots, thereby additionally confirming that PPD molecules are likely to have been immobilized onto the CdSe QD surface.[3]

In terms of other noticeable peaks, aromatic ligands such as PPD and ATP give rise to characteristic peaks for aromatic rings near the 1530-1600 cm^{-1}, 1400-1500 cm^{-1},

and 1160-1175 cm^{-1} regions for the C=C asymmetric stretching mode, the C=C symmetric stretching mode, and the C-H bending mode, respectively. In the AET and ATP-capped CdSe QDs, the peak located at 750 cm^{-1} can be ascribed to the C-S stretching mode.[7] The broad OH vibration peak located at 3430 cm^{-1} and found in the AET-CdSe QDs likely emanates from water. Water adsorbs onto the surfaces of CdSe quantum dots, because of their high surface area-to-volume ratio. The bands located at around 2925 cm^{-1} and 2850 cm^{-1} in the ligand-exchanged QDs can be assigned to a C–C–H stretching mode, implying that there are still small, remnant amounts of TOPO immobilized onto the surfaces of the CdSe QDs, even after the ligand exchange process.

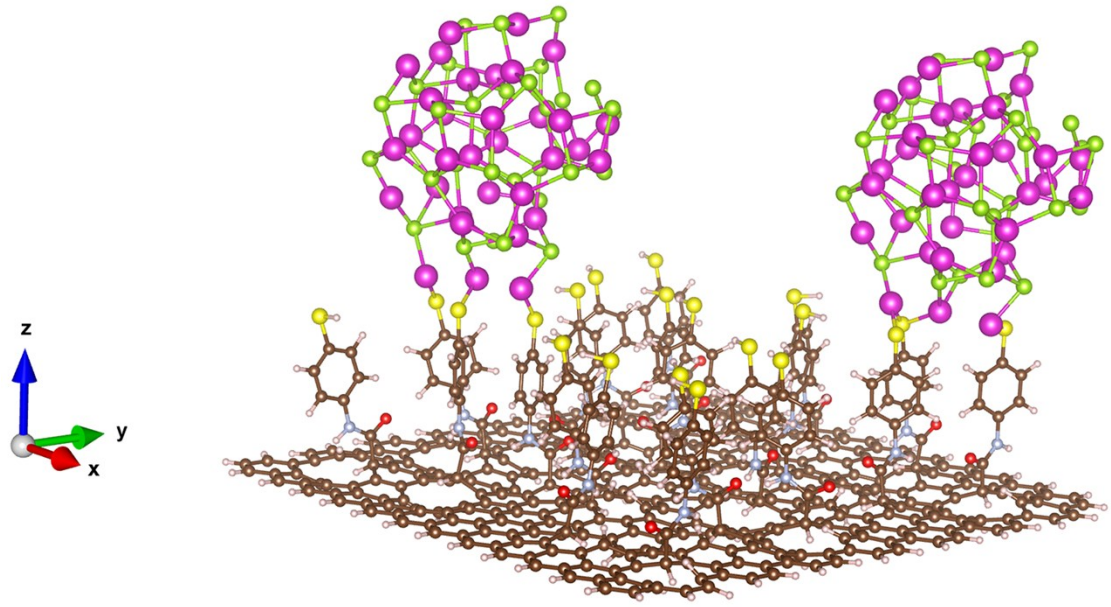

Figure S4. Representative model used in theoretical NEXAS calculations of typical graphene-bound ATP-CdSe QD heterostructures. The atoms are labeled as follows: brown - carbon; white – hydrogen; red – oxygen; gray – nitrogen; yellow – sulfur; pink – cadmium; and green - selenium.

Construction of theory models:

A flat graphene sheet measuring 3 nm x 3 nm and a carbon - carbon bond length of 1.418 Å was created using the VMD software.[8] The sheet was hydrogen terminated using the Avogadro software.[9] The 'defected' system was created from this graphene sheet by adding in 20 defects, randomly spaced around the interior of the sheet. The localized geometries of the 'defected' carboxyl groups as well as that of the local environment in the graphene sheet were each individually allowed to relax using Avogadro's force field optimization with the UFF force field. The linker molecules were subsequently built into this 'defected' system, with the linker molecules attached at the same 'defected' sites in the graphene sheet. Identical relaxation techniques were also applied to the various atoms in the ligands, followed by a geometry relaxation using

NWChem for all systems. Detailed coordinates of each ligand-bound graphene system can be found in separate 'xyz' files, attached herein.

For systems with a CdSe quantum dot, the dot was generated as follows: a würtzite[10] unit cell with a stoichiometric ratio of 1:1 cadmium to selenium was replicated many times along each spatial dimension. Then all atoms outside the desired radius of 0.75 nm were discarded. A sphere of $(CdSe)_{33}$ (i.e. a magic number[11]) was subsequently attached to either the relevant S or N atom after removing the capping hydrogen atom of the linker, and the entire system was subsequently relaxed in NWChem using the identical parameters, as stated above. Full images of these systems, captured in Vesta, are displayed in Figure S4.

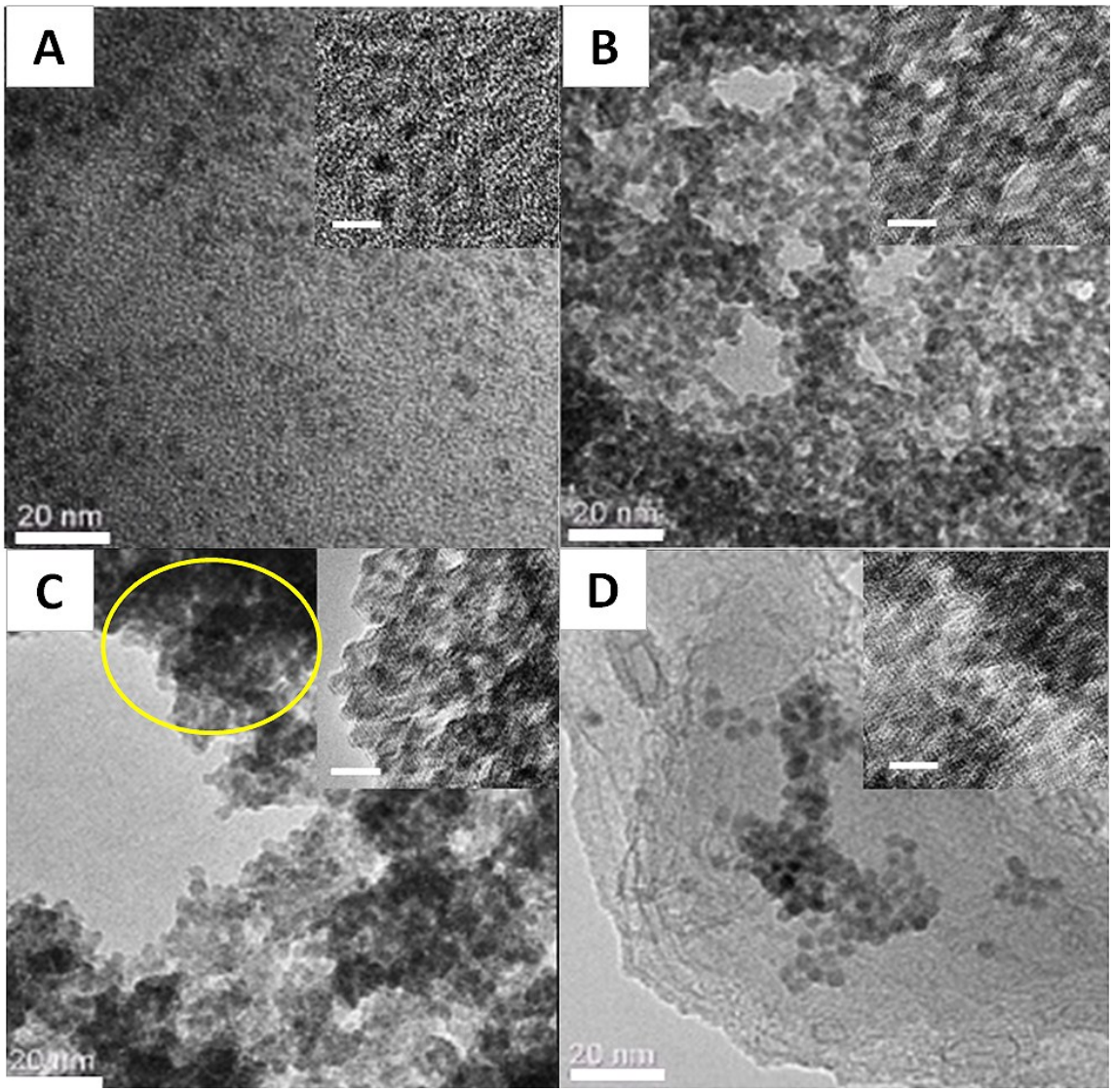

Figure S5. TEM images of (A) as-prepared, (B) PPD-capped, (C) AET-capped, and (D) ATP-capped CdSe QDs, respectively. Insets highlight the corresponding HRTEM images. The scale bars in the insets are 5 nm. The presence of aggregated AET-capped CdSe QDs is emphasized by the yellow circle.

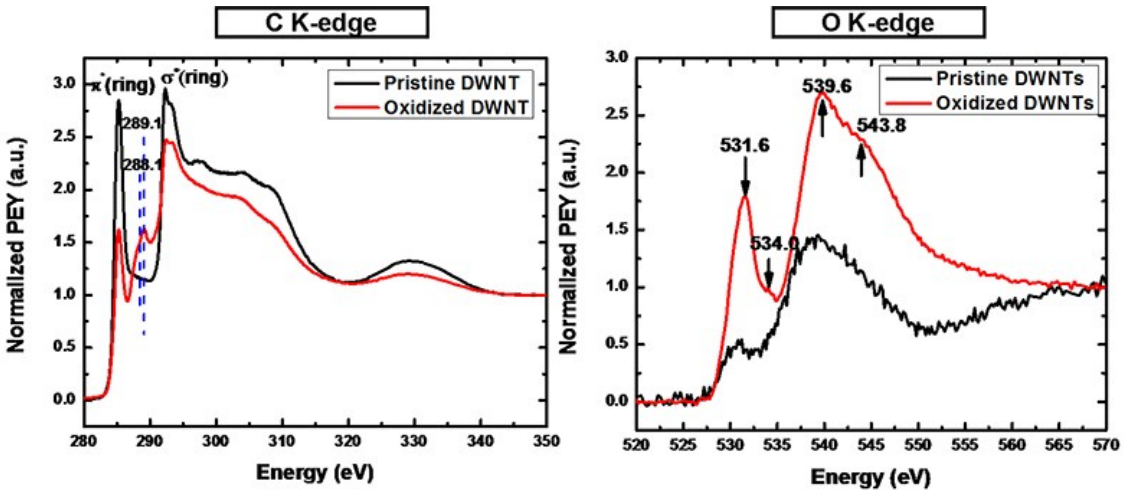

Figure S6. C *K*-edge and O *K*-edge NEXAFS spectra of pristine and oxidized DWNTs.

NEXAFS Data

C *K*-edge data gave rise to prominent transitions at 285 eV, 292-294 eV, and 301–309 eV, respectively, corresponding to a sharp C 1s to C=C π* (ring) transition, three C 1s to C-C σ* (ring) transitions,[12, 13] as well as broad (π + σ) transitions, respectively.[14] After oxidation of the DWNTs, specific transitions at ~288.1 and 289.1 eV, which can attributed to the π* states of carbonyl groups associated with –COOH as well as of σ* states associated with C-O functionalities,[15] became more prominent.

The corresponding O *K*-edge data associated with the oxidized DWNTs evinced several distinctive peaks. Specifically, the peak at 531.6 eV corresponds to the C=O π* transition, which originates from the carbonyl oxygen atom, while the peak at 534.8 eV can be assigned to the "-OH" moiety from the carboxylic group. The two broader peaks located at 539.6 and 543.8 eV can be ascribed to the presence of inequivalent σ* C-O bonds within the carboxylic acid group.[14, 16]

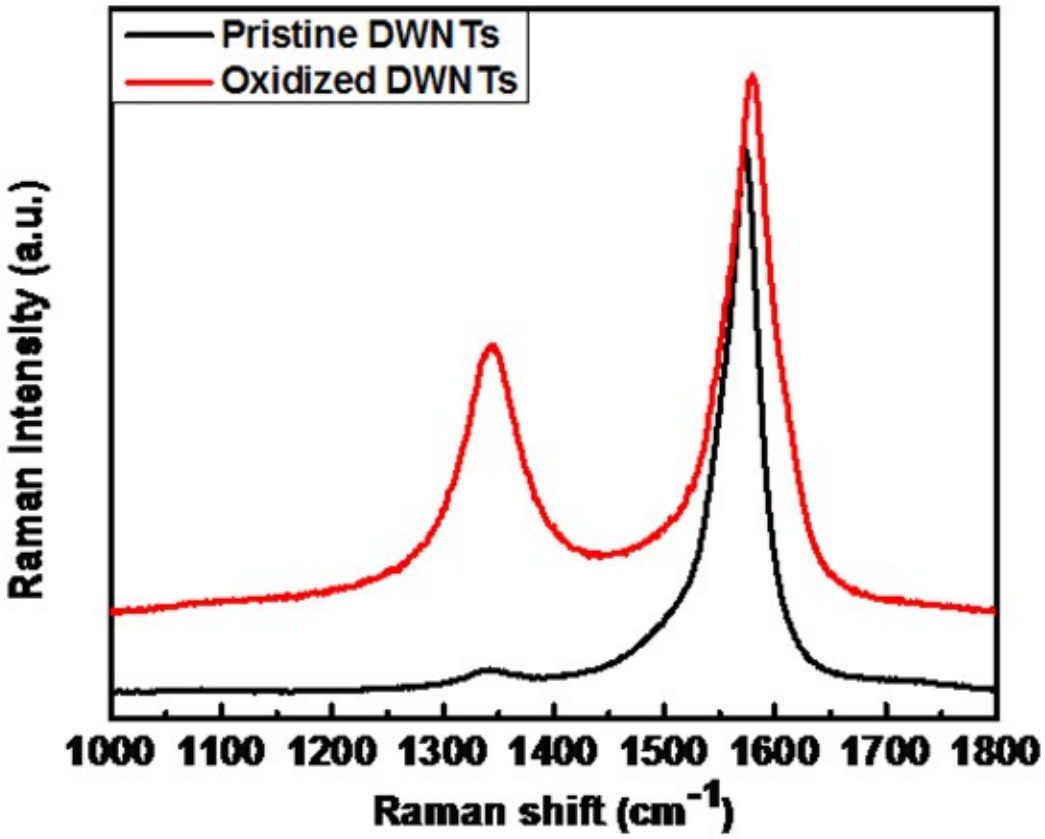

Figure S7. Raman D and G-band data of pristine (black) and oxidized (red) DWNTs, respectively.

References

1. L. Qu and X. Peng, *J. Am. Chem. Soc.*, 2002, **124**, 2049-2055.
2. B. Shakeri and R. W. Meulenberg, *Langmuir*, 2015, **31**, 13433-13440.
3. B. von Holt, S. Kudera, A. Weiss, T. E. Schrader, L. Manna, W. J. Parak and M. Braun, *J. Mater. Chem.*, 2008, **18**, 2728-2732.
4. I. S. Liu, H.-H. Lo, C.-T. Chien, Y.-Y. Lin, C.-W. Chen, Y.-F. Chen, W.-F. Su and S.-C. Liou, *J. Mater. Chem.*, 2008, **18**, 675-682.
5. J. E. B. Katari, V. L. Colvin and A. P. Alivisatos, *J. Phys. Chem.*, 1994, **98**, 4109-4117.
6. A. G. Young, A. J. McQuillan and D. P. Green, *Langmuir*, 2009, **25**, 7416-7423.
7. C. N. R. Rao, R. Venkataraghavan and T. R. Kasturi, *Can. J. Chem.*, 1964, **42**, 36-42.
8. W. Humphrey, A. Dalke and K. Schulten, *J. Mol. Graphics*, 1996, **14**, 33-38.
9. M. D. Hanwell, D. E. Curtis, D. C. Lonie, T. Vandermeersch, E. Zurek and G. R. Hutchison, *J. Cheminformatics*, 2012, **4**, 17-33.
10. Y. N. Xu and W. Y. Ching, *Phys. Rev. B*, 1993, **48**, 4335-4351.
11. A. Kasuya, R. Sivamohan, Y. A. Barnakov, I. M. Dmitruk, T. Nirasawa, V. R. Romanyuk, V. Kumar, S. V. Mamykin, K. Tohji, B. Jeyadevan, K. Shinoda, T. Kudo, O. Terasaki, Z. Liu, R. V. Belosludov, V. Sundararajan and Y. Kawazoe, *Nat. Mater.*, 2004, **3**, 99-102.
12. C. Liu, S. Lee, D. Su, Z. Zhang, L. Pfefferle and G. L. Haller, *J. Phys. Chem. C*, 2012, **116**, 21742-21752.
13. Z. Wang, L. Wu, J. Zhou, W. Cai, B. Shen and Z. Jiang, *J. Phys. Chem. C*, 2013, **117**, 5446-5452.
14. S. Banerjee, T. Hemraj-Benny, M. Balasubramanian, D. A. Fischer, J. A. Misewich and S. S. Wong, *ChemPhysChem*, 2004, **5**, 1416-1422.
15. A. Kuznetsova, I. Popova, J. T. Yates, M. J. Bronikowski, C. B. Huffman, J. Liu, R. E. Smalley, H. H. Hwu and J. G. G. Chen, *J. Am. Chem. Soc.*, 2001, **123**, 10699-10704.
16. V. Leon, R. Parret, R. Almairac, L. Alvarez, M. R. Babaa, B. P. Doyle, P. Ienny, P. Parent, A. Zahab and J. L. Bantignies, *Carbon*, 2012, **50**, 4987-4994.